INTRACELLULAR pH AND IONIC CHANNELS IN THE *LOLIGO VULGARIS* GIANT AXON

EMILIO CARBONE, PIER LUIGI TESTA, AND ENZO WANKE, *Istituto di Cibernetica e Biofisica, Consiglio Nazionale delle Ricerche, Camogli (Genova), 16032, Italy*

ABSTRACT Squid giant axons were used to investigate the reversible effects of intracellular pH (pH_i) on the kinetic properties of ionic channels. The pharmacologically separated K^+ and Na^+ currents were measured under: (*a*) internal perfusion, (*b*) enzymatic Pronase treatment, and (*c*) continuous estimate of periaxonal ion accumulation. Variations of internal pH from 4.8 to 11 resulted in: (*a*) a decrease of steady-state sodium inactivation at positive potentials similar to the effect of the proteolytic enzyme Pronase, (*b*) a shift of the $h_\infty(E)$ curve toward depolarizing voltages, and (*c*) a decrease of the time constant of inactivation for potentials below -20 mV (an increase above). A plot of the steady-state sodium conductance at $E = +40$ mV as a function of pH_i suggests that two groups with pK_a 10.4 and 5.6 affect respectively the inactivation gate and the rate constants for the transition from the inactivated to the second open state (h_2) (Chandler and Meves, 1970*b*). The voltage shifts of the kinetic parameters predicted by the Gouy-Chapman-Stern theory are well satisfied at high pH_i and less at low. Once corrected for voltage shifts, the forward rate constants for channel opening were found to be slowed with the acidity of the internal or external solution.

INTRODUCTION

The action of external hydrogen ions on the ionic currents of various cell membranes has been widely investigated (Hille, 1968; Mozhayeva and Naumov, 1970; Woodhull, 1973; Drouin and Neumcke, 1974; Shrager, 1974; Campbell and Hille, 1976; Schauf and Davis, 1976; Ohmori and Yoshii, 1977; Carbone et al., 1978). In spite of this, little information is available as to the effects of altering the pH of intracellular solutions (pH_i) (Chandler and Meves, 1965; Ehrenstein and Fishman, 1971; Nonner et al., 1980). In the squid axon findings are limited to the existence of three groups: one controlling Na-inactivation gating (Brodwick and Eaton, 1978), one modulating the open K^+ channel conductance (Wanke et al., 1978, 1979), and one blocking in a voltage-dependent manner the open Na^+ channel (Wanke et al., 1980).

We report here detailed studies of the action of pH_i on the properties of ionic channels in the squid axon membrane. Since they were most impressive, the effects on sodium inactivation were studied first with a classical sequence of voltage-clamp measurements: h_∞, τ_h, and then steady-state conductance as a function of membrane potential. Secondly, we studied the action of pH_i on the activation kinetics of Na conductance in terms of the rate constant of channel opening. Finally, to complete the set of results on the pH effects already published (Carbone et al., 78; Wanke et al., 1979, 1980) we also measured τ_h at various extracellular pH (pH_o) and both g_K and α_n at very low values of pH_i and pH_o.

Dr. Wanke's present address is the Istituto di Fisiologia Generale, Università di Ferrara, 44100 Ferrara, Italy.

The whole series of experiments gave us the possibility of drawing some tentative conclusions as to the effect of pH on the membrane of the squid axon which seems at present the sole nerve preparation in which a complete set of data is available. In particular, we found evidence for the presence of two groups with very different pK_a which allow selectively, either removal or closure of the inactivation gate. The data relative to the forward rate constants of both K^+ and Na^+ channels are consistent with the idea that H^+ ions act on the activation gates by either altering the channel-sensed electric field (as a result of a surface-charge density variation) or changing the free energy level associated with the rate constant.

MATERIALS AND METHODS

Axon Chamber and Voltage Clamp

All experiments were performed on isolated segments of giant axons with the squid *Loligo vulgaris* (available in Camogli, Italy). The cleaning and axon-mounting procedure as well as the internal electrode assembly were similar to those described previously (Carbone et al., 1978; Wanke et al., 1979). Axons were internally perfused according to a modified version of the Tasaki method (Armstrong et al., 1973) and bathed in continuously flowing extracellular solutions. The axon chamber was similar to that of Armstrong et al., 1973), except for the central and guard electrodes which were two semicylindrical platinized silver blocks of 8 and 5 mm length, respectively. Two 3-mm wide air gaps were used on each side of the space clamp region. Inside the two semicylindrical regions, three small holes were allocated for: (*a*) a bead-thermistor (0.25 mm), (*b*) the external Ag/AgCl voltage electrode, and (*c*) the inflow of external solutions. The temperature of the bath was measured by the thermistor and controlled by a Peltier cell in direct contact with the silver block through a feedback system. Except when mentioned, all experiments were done at 2 ± 0.1°C.

The voltage clamp apparatus uses field effect transistor (FET) hybrids and integrated circuits; the open loop gain was adjusted in order to have good DC control. The phase shift was compensated to allow both a relatively slow settling time (30 μs) and the possibility of an almost complete elimination of the series resistance (90%). The series resistance itself was measured with a brief pulse of current each time the ionic content of the internal and external solutions was changed (Binstock et al., 1975). Details on data acquisition and storage as well as on the method used to measure the time-course of K^+ conductance avoiding the effects of K^+ ion accumulation in the periaxonal space (Frankenhaeuser and Hodgkin, 1956) have been given elsewhere (Wanke et al., 1979).

At rest, fibers were usually held at a membrane potential of -60 to -70 mV and preconditioned to -90 mV for 1–2 min before stimulation. In experiments were Na^+ currents were investigated, removal of slow sodium inactivation (Chandler and Meves, 1970 *d*) was accomplished by preconditioning the fiber to -90 mV for at least 180 s before a pulse series and to -130 mV for 0.5 to 1 s between successive stimuli. When strong depressions of I_{Na} were observed, tetrodotoxin-insensitive currents were subtracted from the total at the end of the experiment. Routinely, current records were corrected analogically and digitally for leakage and capacitative components.

For most experiments $h_\infty(E)$ was measured by the two-pulse procedure described by Bezanilla and Armstrong (1977). Conditioning prepulses were 40-ms long and varied from -90 to $+90$ mV. Test potentials were either $+40$ or 0 mV depending on whether axons were perfused respectively with 200 or 50 Na-standard internal solution (SIS) (Table I). The brief hyperpolarization delivered between the offset of the conditioning and the onset of the test pulse lasted 0.9 ms and took E_m to -90 mV. Measured in this way, $h_\infty(E)$ at negative potentials has the same voltage dependence as determined by conventional methods (Hodgkin and Huxley, 1952 *a*). For membrane potentials below -30 mV the time-course of inactivation was measured following the two-pulse procedure adopted by Hodgkin and Huxley (1952 *a*). Above -40 mV, τ_h was determined by curve fitting the time-course of sodium currents, $I_{Na}(t)$, after a Hodgkin and Huxley type of analysis.

TABLE I

IONIC COMPOSITION OF THE SOLUTIONS

External Solutions, *mM*									
	Na^+	K^+	TMA	Chol.	Tris	Ca^{2+}	Mg^{2+}	Cl^-	pH (± 0.1)
ASW	435	10			20	10	40	555	8
1/4 NaSW TMA	109	10	326		20	10	40	555	8
1/4 NaSW Chol	109	10		326	20	10	40	555	8

Internal solutions, *mM*								
	Na^+	K^+	Cs^+	F^-	$H_2PO_4^-$	Citrate	Glutamate	pH (± 0.1)
50 NaSIS	50	135	215	317	45			7.2
200 NaSIS	200			117	45			7.2
200 Na (pH 10)	200			130			45	10
200 Na (pH 5.5)	200			80		45		5.5
400 KSIS		400		317	45			7.2

Solutions

The ionic composition of the solutions employed are reported in Table I. Internal solutions were prepared with fluoride as the main anion. Phosphate and glutamate, which are the anions usually employed for internal perfusion studies (Tasaki et al., 1965), were used as pH-buffers at a concentration of 45 mM. This, however, did not produce appreciable distortions as to the effects of pH_i on ionic currents. Solutions of different pH_i had the same buffer concentration (45 mM) and Na^+ or K^+ content, depending whether Na^+ or K^+ currents were studied. Sucrose was added to adjust the osmolarity to 1,070 mosmol. The amount and the type of buffers used was already established in a previous work (Wanke et al., 1979). When required, fast sodium inactivation was removed by perfusing the fiber for 30–60 s with 400 KSIS at pH 9–10 containing 1 mg/ml Pronase (Calbiochem, Behring Corp., American Hoechst Corp., San Diego, Calif.). This procedure speeded up the rate of inactivation removal without much affecting the peak amplitude of the sodium records (Carbone and Wanke, manuscript in preparation).

Axons were usually perfused with 200 NaSIS and bathed in 1/4 Na-sea water (SW) tetramethylammonium (TMA) or Choline. This allowed: (*a*) the use of ohmic relations to calculate the sodium conductance, g_{Na}, instead of using the Goldman-Hodgkin-Katz equation to derive sodium permeability, (*b*) reduced the errors due to series resistance, and (*c*) avoided distortions due to K^+-channel blocking ions. On the contrary, it prevented reliable g_{Na} measurements at low depolarizing voltages near the sodium equilibrium potential ($E_{Na} = -15$ mV). Membrane voltages were not corrected for liquid-junction potentials.

Data Analysis

For computational reasons the forward rate constants of the Na^+-activation process was determined in terms of the Armstrong and Bezanilla model (AB) (1977), not inclusive of the second open state h_2. Channels were assumed to be in state x_4 at $t = 0$ and rate constant λ to be equal to zero for $E_m > 0$ (E_m, membrane potential in absolute units). Qualitatively similar results were obtained in terms of the classical Hodgkin and Huxley model (1952 *b*). In the range of potentials explored (0 to +110 mV), only the forward rate constant, $a(E)$, was considered to be meaningful and, thus, reported. At positive voltages the backward rate, $b(E)$, was found to be small and affected by large errors.

The time-course of K^+ conductance, $g_K(t)$, was analyzed in terms of the Hodgkin and Huxley equations (1952 *b*) assuming for n a constant exponent equal to four and n_∞ (E_h) = 0 (E_h, holding potential). As for the sodium kinetics, data on β_n are not reported.

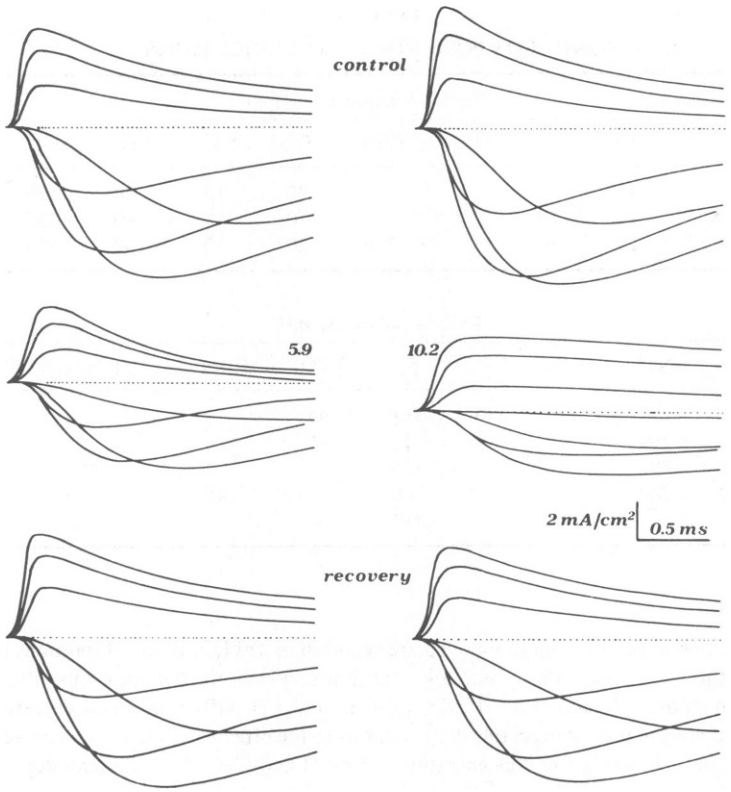

FIGURE 1 Sodium current density records from two axons at low and high pH_i · V_h −90 mV. Step depolarizations were respectively: −30, −10, +10, +30, +70, +90 and +110 mV. The internal solution was 50 NaSIS containing 45 mM K-glutamate (pH 10.2) or 45 mM K-phosphate (pH 5.9). Out: artificial sea water (ASW).

The method used to determine the horizontal and vertical shifts of $a(E)$, $\alpha_n(E)$, $g_{Na}(E)$ and $g_K(E)$ at high and low pH_i was empirical and based on a curve-fitting analysis done manually. A continuous curve was drawn by eye through control data at pH_i 7.2 and than moved along the horizontal and vertical axis until a good fitting of the test pH points was obtained. The final displacements were estimated and reported on the figures with a corresponding arrow. Although quite subjective, the uncertainty of the method did not exceed 4–6 mV for the horizontal shift and 5–10% for the vertical displacement.

RESULTS

General Observations

Variations of internal pH result in a rapid modification of the fast inactivation process of sodium channels, as illustrated in Fig. 1. In the presence of 215 mM Cs^+ to block delayed ionic currents, low pH_i produces a reduction of peak I_{Na} and a stronger depression of the residual steady-state level. On the contrary, high pH_i removes sodium inactivation and depresses peak sodium currents, resembling partly the action of the proteolytic enzyme Pronase (Armstrong et al., 1973). pH effects are usually complete within 30–40 s and reverse

to 90% of the initial conditions upon returning to control pH. In both cases no appreciable variations of E_{Na} are observed.

One of the questions which arose during the course of the investigations was whether the presence of Cs^+ (or other K^+-channel blocking agents) might affect the action of internal pH on sodium currents. In *Myxicola* axons, internal Cs^+ alters Na-inactivation (Schauf and Bullock, 1978) whereas in the squid tetraethylammonium (TEA^+) depresses more efficiently Na^+ channels which have been previously treated with Pronase (Rojas and Rudy, 1976), as if removal of the inactivation gates increases the affinity of TEA^+ toward the channel. Our personal observation is that in normal axons at pH_i 7.2 internal Cs^+ decreases the steady-state Na conductance and accelerates the time-course of fast inactivation. In Pronase-treated fibers, Cs^+ reduces by 10–20% the magnitude of the sodium current. Thus, to avoid any interference of Cs^+, test pH experiments were carried out with solutions in which Cs^+ and K^+ were replaced with Na^+. As shown in Fig. 2, the two families of curves present strong similarities with those of Fig. 1, i.e., sodium inactivation is almost completely removed at pH

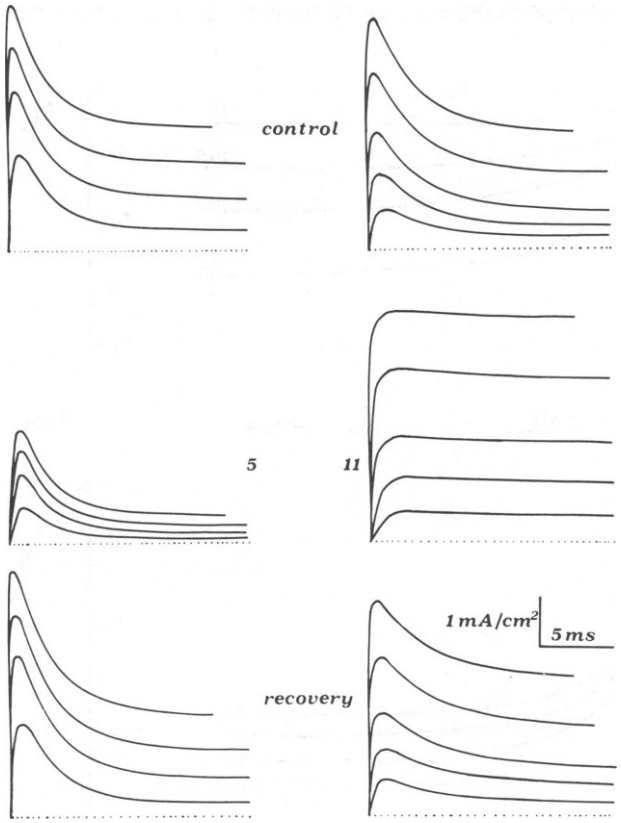

FIGURE 2 Sodium current density records at pH_i 5 and 11 in the absence of internal Cs^+. Records are taken from different axons. V_h −90 mV. Step depolarizations were to: +40, +70, +90, and +110 mV at low pH_i and +10, +30, +50, +80, and +110 mV at high pH_i. Records were corrected by subtracting tetrodotoxin (TTX) insensitive currents. In: 200 NaSIS. Out: ¼ NaSW TMA.

11 and enhanced at pH 5. In 10 fibers perfused at high pH_i, peak amplitude increases similar to that in Fig. 2 (5–20%) were consistently observed. Occasionally, at pH_i higher than 10 axons with high resting potential and low leakage conductance could have peak sodium currents as much as 30% greater than the original value. No such changes could be detected in Pronase-treated axons.

The effects of pH_i on I_{Na} are more evident from the results of Fig. 3. pH_i variations from 7.2 to 11 result in an increase of the normalized steady-state level (I^{ss}_{Na}/I^{p}_{Na}) while the time-course of sodium inactivation is prolonged (see Fig. 3, right). Lowering pH_i from 7.2 to 5.4 results in a potentiation of the sodium inactivation which partly resembles the action of internally applied *n*-alkanols (Oxford and Swenson, 1979). At $E = +40$ mV, I^{ss}_{Na}/I^{p}_{Na} decreases from 0.28 to 0.1 without remarkable effects on the decay time constant (Fig. 3, bottom).

A plot of the normalized I^{ss}_{Na} at various pH_i (filled circles) is given in Fig. 4. On the ordinate are reported I^{ss}_{Na} values at $E_m = +40$ mV which were scaled up so that the amplitude of the peak current matched that of the control records. Scaling corrects for the block by hydrogen ions at low pH_i (Wanke et al., 1980) and for the slight increase of peak conductance at high pH_i. Data are all referred to the average I^{ss}_{Na} at pH 7.2, 0.26 ± 0.1 times I^{p}_{Na} (open square).

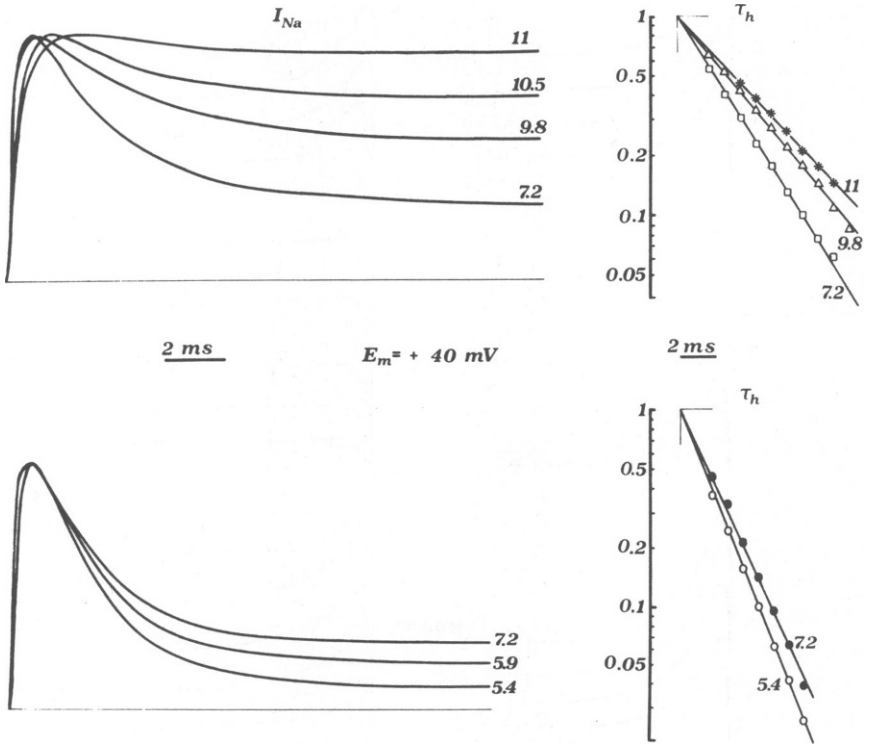

FIGURE 3 Normalized I_{Na} records at various pH_i. Left: records taken from five different axons and scaled in amplitude to match the peak value of the control curve at $E_m = +40$ mV. Normalization factors are: 0.97 (pH 9.8), 1.2 (10.5), 1.12 (11), 1.54 (5.4), and 1.3 (5.9). Right: Semilog plots of the decaying part of the I_{Na} records. Symbols are experimental points. Straight lines are the results of a least-square fitting. Records were corrected for TTX-insensitive currents. In: 200 NaSIS. Out: ¼ NaSW TMA.

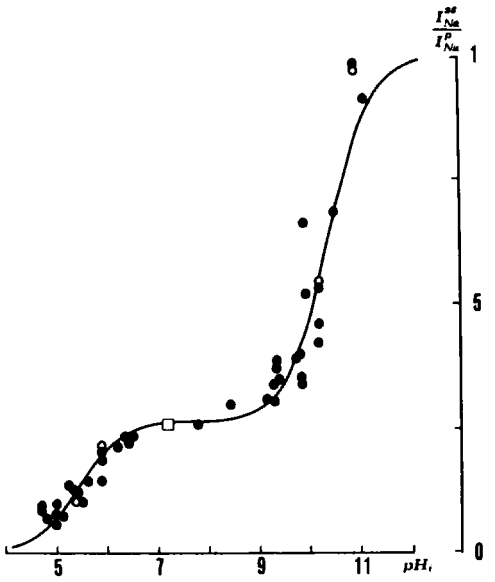

FIGURE 4 Normalized I_{Na}^{ss} (●) and h_∞ (○) as a function of pH_i. Data points represent test pH measurements taken from 33 axons perfused either with 50 or 200 NaSIS. The □ indicates the average of the control I_{Na} values (see text). The continuous curve is the result of a least-square fitting according to Eq. 4 in the Appendix for $I'_{Na}/I_{Na} = 0.27$, $pK_a = 5.4$ and $pK_b = 10.4$.

The solid curve drawn through the data points represents the results of a least-squares analysis based on Eq. 4 in the Appendix (Discussion).

Effects of pH_i on $h_\infty(E)$

The effects of internal pH on the sodium inactivation parameter $h_\infty(E)$ are illustrated in Fig. 5. Curves are normalized at $E = -90$ mV and show the characteristic S-shaped voltage dependence with residual values between -20 and $+90$ mV. During high pH_i exposure, $h_\infty(E)$ increases with the pH. At pH_i 10.9 steady-state inactivation ($1\text{-}h_\infty(E)$) is close to zero and practically voltage independent whereas at intermediate values (9.8 and 10.5), $1\text{-}h_\infty(E)$ increases from 0 to 0.6 or 0.25. No detectable shifts were observed as estimated by the position of the midpoint potential, $E_{1/2}$, defined as the potential at which h_∞ is half the difference between its maximum and minimum value.

Under low pH_i treatment, $h_\infty(E)$ decreases with pH in the voltage-independent region and shifts toward negative potentials. Evaluated from $E_{1/2}$ the pH dependence of the shifts (ΔV) are shown to the right of Fig. 5. The solid line represents the result of a curve fitting (see figure legend for details). Interestingly values of h_∞ at $E_m = +40$ mV obtained at different pH_i have a pH dependence similar to I_{Na}^{ss}, as shown in Fig. 4 (open circles).

Inactivation Time Constant and pH_i

Two major features should be stressed about the action of pH_i on the time constant of inactivation (Fig. 6 *a*). First, intracellular pH drastically affects the amplitude of the bell-shaped curves without appreciably affecting their peak position. Second, the effect of pH_i

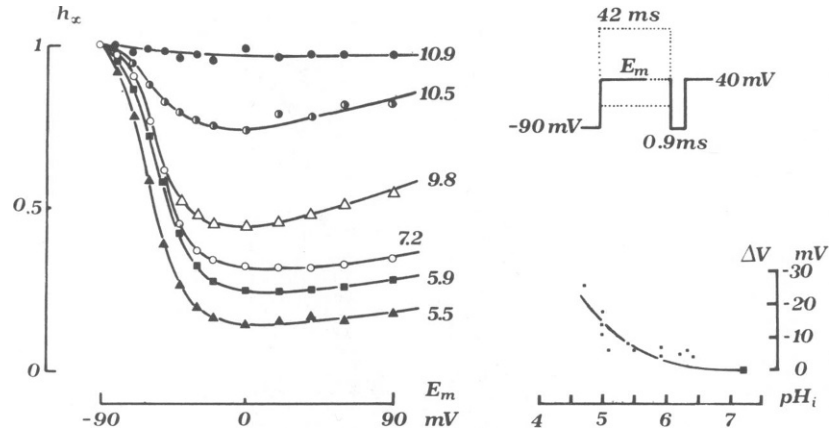

FIGURE 5 Left: Steady-state inactivation curve $h_\infty(E)$ at various pH_i as determined with a double-pulse method (Bezanilla and Armstrong, 1977). The pulse procedure is indicated in the inset. Ordinate: normalized peak sodium current at $E_m = +40$ mV. Abscissa: membrane potential during conditioning prepulse. Continuous curves were drawn by eye to best fit the experimental points. Records were corrected for TTX-insensitive currents. In: 200 NaSIS. Out: ¼ NaSW TMA. Similar results were obtained also from axons perfused with solutions containing Cs^+ and K^+ (50 NaSIS). Right: pH-dependence of the voltage shift as determined from $E_{1/2}$ (see text). Dots represent experimental points obtained from different axons. The solid line is the result of a curve-fitting analysis based on the following equation (Gilbert and Ehrenstein, 1969; Mozhayeva and Naumov, 1970; Hille et al., 1975):

$$\sigma_1(1 + \gamma[H]_o/K_1)^{-1} + \sigma_2(1 + \gamma[H]_o/K_2)^{-1} - \sigma_3(1 + K_3/\gamma[H]_o)^{-1} = C\left[\sum_{i=1}^{m} c_i(\gamma^{z_i} - 1)\right]^{1/2},$$

where $\gamma = e^{F(B-E_{1/2})/RT}$; F, R, T, have the usual meaning and B is an arbitrary constant determining reference for potential shifts; K_1, K_2, and K_3 are the dissociation constants regulating first-order reactions between hydrogen ions and fixed surface charges (K_1 and K_2 refer to acid groups and K_3 to a basic group); σ_1, σ_2, and σ_3 are the corresponding total charge densities; $[H]_o$ is the concentration of H^+ in bulk; m is the number of ionic species; c_i and z_i are respectively the concentration and the valence of ionic species i; C is a constant at a given temperature. The line was obtained by setting: $B = 20$ mV, σ_1, σ_2, and σ_3, respectively 4, 3.5, and 6×10^{-3} electronic charges: $Å^{-2}$, K_1, K_2, and K_3, respectively 0.31×10^{-4}, 0.16×10^{-2}, 0.13×10^{-9} M to which corresponds a pK_a of 4.5, 2.8, and 9.9.

reverses at about −20 mV. pH_i 10.2 produces a reduction of τ_h in the range −90 to −20 mV but an increase from −20 to +90 mV. Opposite effects are observed at low pH_i. For comparison, in Fig. 6 *b* are reported the effects of external pH (pH_o) on τ_h which extend previous observations by Carbone et al., 1978. At low pH_o the peak amplitude of the bell-shaped curve increases and shifts to the right (Courtney, 1979).

Effects on $g_{Na}(E)$

Fig. 7 summarizes the results of measurements on peak (g^p_{Na}) and steady-state (g^{ss}_{Na}) sodium conductances extended to very large voltages at high (*a*) and low pH_i (*c*). In agreement with Chandler and Meves (1970 *a*), g^p_{Na} and g^{ss}_{Na} show remarkably different voltage dependences at control pH (circles). Peak conductance is a steep function of voltage (8–10-mV potential

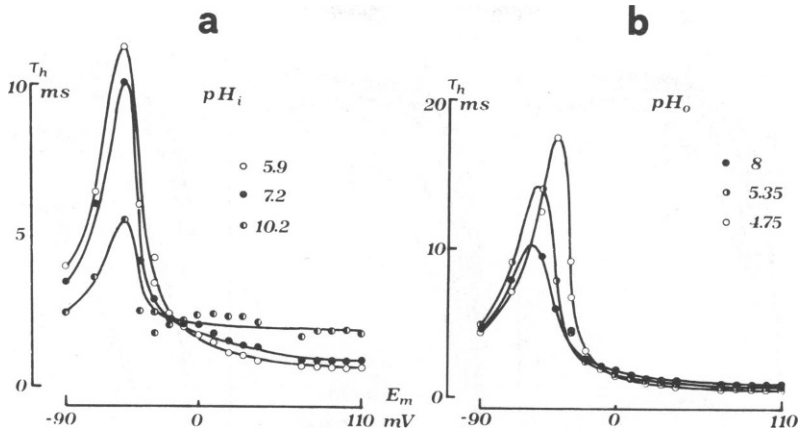

FIGURE 6 Time constant, τ_h, vs. E_m at various pH_i and pH_o. For details of the procedure see Methods. Lines through experimental points (circles) were drawn by eye. Note the different scale of the ordinates. In: 50 NaSIS. Out: ASW. Compared with other τ_h curves in the literature, e.g., Fig. 3 in Chandler et al., 1965, our τ_h curves at pH_i 7.2 appear lower and slightly shifted toward depolarizing voltages. This might be due to different perfusion conditions (300 mM KCl against 215 mM CsF, see Schauf and Bullock, 1978).

change for an *e*-fold increase) whereas g^{ss}_{Na} is less voltage sensitive, requiring a 40–50-mV potential variation for an *e*-fold change. Incidentally, the slight bend of g^{ss}_{Na} above 150 mV was somehow unexpected and not further investigated in the present paper.

At high pH_i (squares) g^{p}_{Na} shifts to the right and g^{ss}_{Na} approaches more closely the peak conductance curve. A plot of the voltage shifts (ΔV) of $g^{p}_{Na}(E)$ vs. pH_i is illustrated in the inset. As shown in Fig. 7*a*, g^{p}_{Na} and g^{ss}_{Na} at pH_i 9.9 have similar voltage dependences at negative potentials and reach approximately equal values at E = 150 mV. Interestingly, the same effects are observed when axons are exposed sequentially to the action of Pronase (Fig. 7 *b*). As the enzyme action approaches completeness (long-lasting digestions) g^{ss}_{Na} tends to g^{p}_{Na}. Such a striking correspondence between the results of Figs. 7 *a* and *b* was taken as strong support for the idea that high pH_i and pronase remove sodium inactivation probably by modifying the same kinetic reaction (Discussion).

Remarkably different are the effects of low pH_i. As shown in Fig. 7 *c*, low pH_i produces appreciable changes in the shape of both g^{p}_{Na} and g^{ss}_{Na}. Above 150 mV at pH_i 5.3 the two curves are seen to increase with potential even though the corresponding quantities at pH_i 7.2 are no longer voltage dependent. Since for g^{p}_{Na} the phenomenon has been interpreted in terms of a voltage-dependent internal block of Na channels by hydrogen ions (Wanke et al., 1980), the present results would suggest that the properties of the block could be also valid at the steady state of g_{Na}.

Na^+ Activation Kinetics and pH_i

In this paragraph attention is focused on the time-course of the Na^+-conductance increase. Fig. 8 shows the effect of PH_i on the rising phase of g_{Na} at E = +110 mV in intact axons (*a*, *d*) and in fibers heavily treated with Pronase to reduce the activation-inactivation coupling

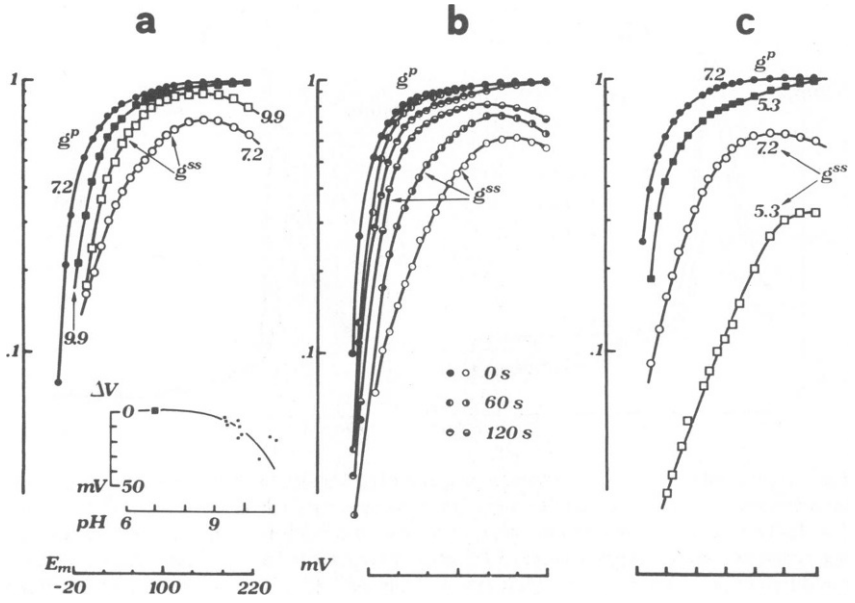

FIGURE 7 Normalized steady-state, g^{ss}, and peak, g^p, sodium conductances vs. E_m at high pH_i (*a*), during Pronase treatment (*b*) and at low pH_i (*c*). *Inset:* voltage shift of g^p_{Na} (ΔV) against pH_i. The solid line is the result of a curve-fitting based on the model illustrated in Fig. 5, using the same set of parameters. $g^{ss}(E)$ curves (○, □) are normalized to the corresponding $g^p(E)$ curve at control pH (●, ■). Normalization factors for g^p were: 1 for pH 9.9, 0.9 for Pronase at 60 s and 1 for 120 s, 1.2 for pH 5.3. In (*b*) are indicated the durations of the enzyme action. Pronase was dissolved in 200 NaSIS at pH_i 9.9 (1 mg/ml). Errors due to accumulation of Na^+ ions in the periaxonal space (Frankenhauser and Hodgkin, 1956) were estimated with the same procedure used for K^+ ions by Wanke et al. (1979) and found to be <5%. TTX-insensitive currents were subtracted before measuring g_{Na}. This avoided the contribution of outward Na^+ currents through K^+ channels which is appreciable at very high voltages (20–30% at $V > 180$ mV) (Bezanilla and Armstrong, 1972; French and Wells, 1977). In: 200 NaSIS. Out: ¼ NaSW Chol.

(*b*, *e*). As shown, both low and high pH_i appear to slow down the rising phase of I_{Na} records regardless of the presence of the fast inactivation process. In spite of this, however, their action on $a(E)$ presents substantial differences. High pH_i merely shifts $a(E)$ along the horizontal axis while low pH_i reduces its amplitude by 50% (see "Data Analysis" for a description of the procedure followed to estimate horizontal and vertical displacements).

Effects on K^+ Channels

The effects of pH_i on the time-course and voltage dependence of potassium conductance have already been reported (Wanke et al., 1979). Referring to those experiments, we report here pH_i effects on the shifts, ΔV, of $g_K(E)$ curves and on the activation rate constant α_n (Fig. 9). Two features in the figure should be stressed. First, ΔV, behaves at high pH_i similarly to the shifts of $g^p_{Na}(E)$ previously described. Second, by comparing Fig. 9*a* with Fig. 3 of Wanke et al. (1979), a clear difference in the pH dependence of ΔV and $\bar{g}_K$ becomes evident, indicating the existence of distinct titratable groups controlling the two quantities.

The behavior of $\alpha_n(E)$ at low pH_i (Fig. 9 *b*) is similar to the observed $a(E)$ curve for Na^+ activation. Slightly different are the effects of high pH_i. At pH_i 9.5, $\alpha_n(E)$ crosses over the

control curve at around +25 mV requiring a 20% vertical shift and a 10-mV voltage displacement to overlap the control data points.

Further Studies on the Effects of Low pH_i and pH_o on g_K.

In an early stage of our work we reinvestigated the effects of low pH_i on maximum potassium conductance, $\bar{g}_K$, to study whether the non-zero conductance at pH_i below 5.2 was due to imperfect buffering of internal solutions (see Fig. 3 of Wanke et al., 1979). To do this, four axons were first extensively treated with Pronase at pH_i 7.2 for 20 min at a concentration of 1 mg/ml and then perfused at pH_i below 5.5. Surprisingly, in all four experiments we obtained reversible $\bar{g}_K$ depressions 50–70% stronger than those previously reported, as if in heavily Pronase-treated fibers pH_i blocks K^+ channels more efficiently, perhaps as a consequence of the reduced amount of residual buffering protoplasm. The possibility that long Pronase

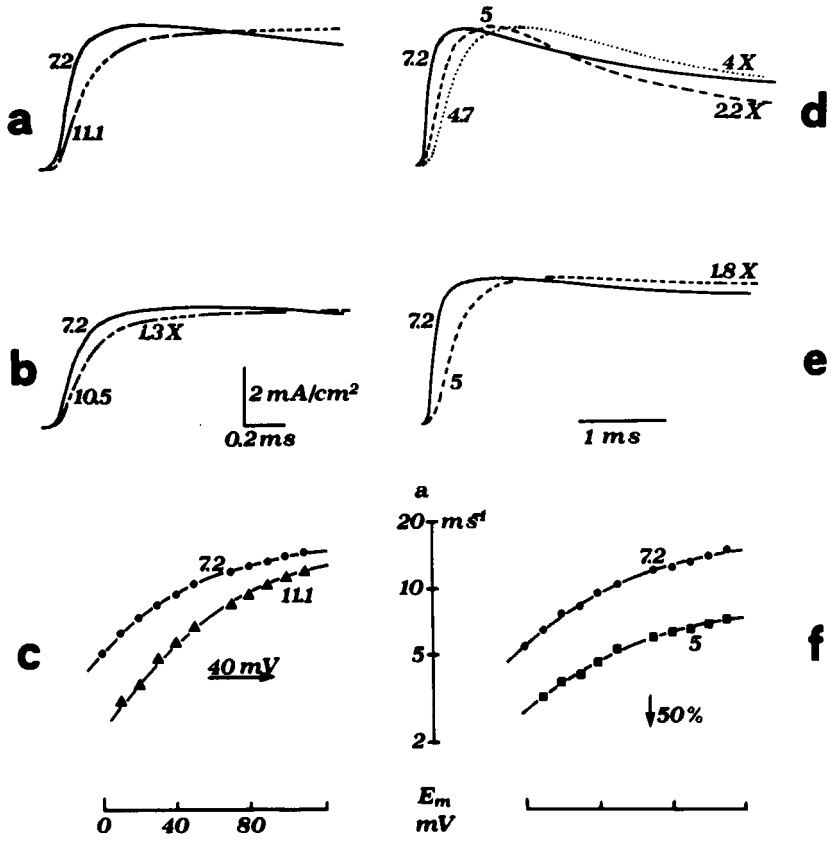

FIGURE 8 Na^+ channels activation kinetics. (*a*, *b*, *d*, and *e*) Normalized time-course of Na^+ currents at high and low pH_i for E_m = 110 mV. Normalization factors are indicated on top of each curve. (*c*, *f*) Forward rate constant *a(E)* obtained according to an AB-fitting analysis of records from intact axons. Arrows indicate vertical and horizontal shifts required to match the control and test-pH curves drawn by eye. Pronase-treated fibers (*b*, *e*) were perfused for 100 s with an enzyme concentration of 2 mg/ml, pH_i 9.9. Current records were corrected by subtracting TTX-insensitive currents. In: 200 NaSIS. Out: ¼ NaSW TMA. Similar results were obtained with axons perfused with 50 NaSIS.

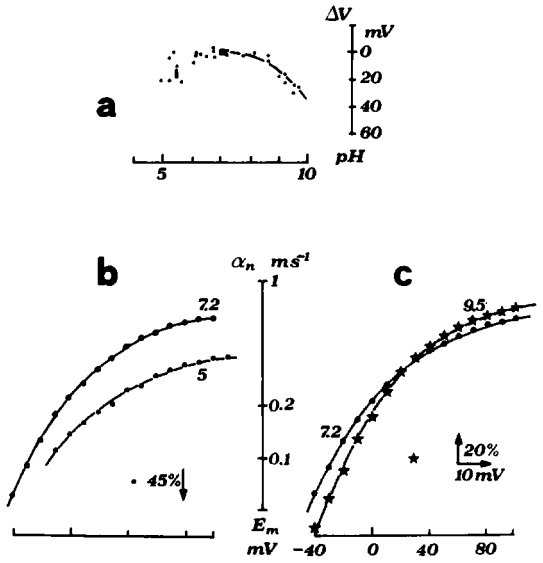

FIGURE 9 (*a*) Internal pH effects on the voltage shift ΔV of $g_K(E)$. The line is the result of a curve-fitting based on the equation given in Fig. 5. Parameters were the same except for K_3 which was 10^{-9}. (*b*, *c*) Forward rate constant vs. membrane potential, $\alpha_n(E)$, obtained according to an HH-fitting analysis at the indicated pH. Arrows represent the horizontal and vertical shifts required to superimpose control and test-pH data. Curves through experimental points were drawn by eye. In: 400 KSIS. Out: ASW + 3 × 10^{-7} M TTX.

digestions could have affected channel properties was ruled out by the observation that the action of the enzyme did not produce appreciable alterations to the voltage dependence of $g_K(E)$ and $\alpha_n(E)$. The implication of these findings is that a large fraction of K^+ channels (<95%) are controlled in an all-or-none manner by a single titratable group with pK_a near 6.4. In a series of six experiments with axons bathed in 300 mM KCl there was evidence that H^+ blockage at low pH_i is independent of the direction of K^+ current flow.

With the present set-up we also extended the g_K measurements of Carbone et al. (1978) to very low pH_o in the absence of internal sodium ions. Below pH_o 4, we could observe excellent reversibility of changes in g_K kinetics accompanied by incomplete recovery of the maximum conductance. A plot of $\bar{g}_K$ as a function of pH_o (not shown) indicated the existence of an acidic group (pK_a near 3.4) affecting the ionic conductance of the channel. In a series of experiments in which pH_i and pH_o were varied simultaneously, the results confirmed the tacit assumption that pH_o and pH_i act independently on the two sides of the membrane.

DISCUSSION

Steady-State Sodium Conductance and pH_i Action

One of the main findings of the present paper is that the steady-state conductance of Na channels might be controlled by the degree of protonation of two titratable groups: tentatively one with pK_a 10.4 and the other with pK_a 5.6. The two groups have well-separated dissociation constants and affect so differently the voltage dependence of g_{Na}^{ss} that it seems safe to assume

different mechanisms of action of the two groups on the kinetics of Na channel. To study the specific effects of those groups in more detail, we analyzed the data in terms of the kinetic model proposed by Chandler and Meves (1970 *b*) or, which is equivalent in our case, by Armstrong and Bezanilla (1977). In this latter model the normal open (x_1) the inactivated (x_1z) and the noninactivated (h_2) states of Na channels are kinetically related as follows:

$$x_1 \underset{\lambda}{\overset{\kappa}{\rightleftharpoons}} x_1 z \underset{\pi}{\overset{\epsilon}{\rightleftharpoons}} h_2, \tag{1}$$

where κ, ϵ, and π are rate constants; x_1 and h_2 are open states with a voltage dependence represented by $g^{p}_{Na}(E)$ and $g^{ss}_{Na}(E)$, respectively. λ is nearly zero at positive potentials (Hodgkin and Huxley, 1952 *b*; Chandler and Meves, 1970 *b*).

According to the above scheme, part of the present results can be tentatively interpreted saying that high pH_i would increase the average number of channels in state x_1 by blocking or affecting the fast-inactivation process (reaction $x_1 \rightarrow x_1z$). This view is supported by the evidence that high pH_i shares common properties with other inactivation-removing agents such as Pronase (Armstrong et al., 1973) and *N*-bromoacetamide (Oxford et al., 1978): (*a*) increasing the steady-state sodium currents (Figs. 1–3), (*b*) decreasing ($1\text{-}h_\infty$) (Fig. 5), and (*c*) modifying $g^{ss}_{Na}(E)$ into $g^{p}_{Na}(E)$ (Fig. 7). The alternative possibility that the increments of g^{ss}_{Na} at high pH_i could be merely due to changes of the rates ϵ and π, either caused by a variation of their voltage dependence or by a voltage shift, is ruled out by the results of Fig. 7. Under these conditions an increase of ϵ with respect to π at high pH_i would certainly produce an increment of the number of channels in h_2 and hence of g^{ss}_{Na}, but it would not modify $g^{ss}_{Na}(E)$ into $g^{p}_{Na}(E)$ as shown in the figure.

The effects of high pH_i differ from those of Pronase in several aspects. They are quick, reversible, and produce alterations in the time constant of the decaying part of I_{Na}. Hence, considering that protonation-deprotonation reactions are fast processes (microseconds at 2°C) with respect to the time scale of channel gating (Atwell and Eisner, 1978), it seems reasonable to assume (Appendix) that at high pH_i there would exist simultaneously two types of channels in rapid equilibrium with each other: one (type C_2) following scheme 1 and one (type C_3) lacking the reaction $x_1 \rightarrow x_1z$. Fluctuations between the two schemes would occur at rates 10^2–10^3 times more rapid than channel gating.

Although less straightforward, the effects of low pH_i on g^{ss}_{Na} can be interpreted according to scheme 1 by saying that in the steady state an increased average number of channels would populate state x_1z. However, on the basis of the present findings we can not discriminate whether low pH_i would simply modify reactions rates κ, ϵ, and π or if more likely (results of Fig. 10) it would inhibit transition $x_1z \rightarrow h_2$, creating channels of type C_1 (Appendix). The results of Fig. 7 *c* would only indicate that low pH_i produces variations of $g^{ss}_{Na}(E)$ which are in agreement with the idea that a voltage-dependent block for g^{p}_{Na} of the type described by Wanke et al. (1980) is also valid at the steady state. Nevertheless, a third possible interaction like the time-dependent ionic block produced by certain pharmacological agents (Yeh and Narahashi, 1977), can be excluded *a priori* by the results of Fig. 8 *e*. Sodium currents from Pronase-treated axons show no significant evidences of an inactivation process at low pH_i indicating that H^+ ions act on state x_1z and/or h_2 rather than becoming an inactivating particle.

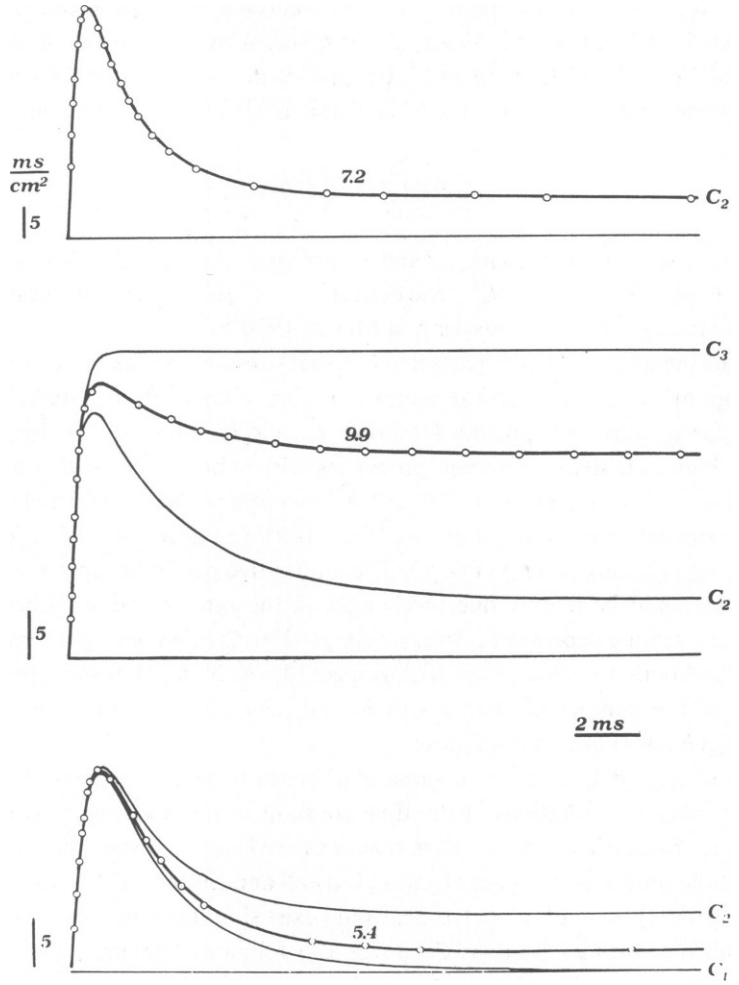

FIGURE 10 Computer simulation of the time-course of g_{Na} at normal (top), high (middle), and low (bottom) pH_i. Dots are experimental g_{Na} values taken from different axons, depolarized from −90 mV to +40 mV. TTX-insensitive currents were subtracted. In: 200 NaSIS. Out: ¼ NaSW. Thin curves illustrate the time-course associated with the kinetic schemes C_1, C_2, and C_3 indicated in the Appendix. Thick lines are the results of the fitting. The value of parameters and the percent of C_1, C_2, and C_3 required to best fit the dots are reported in Table II. Referring to the assumptions described in the Appendix, curve fittings were carried out by postulating that: (*a*) the total number of channels is constant at any time, $x_3 + x_2 + x_1 + x_1 z + h_2 = N$, (*b*) all channels are in state x_3 at $t = 0$ and (*c*) $g_{Na} = \bar{g}_{Na}(x_1 + h_2)$ where $\bar{g}_{Na}$ represents the conductance of the open channel times N. To limit our fitting to four adjustable parameters: $\bar{g}_{Na}$, a, b, and ϵ/π, we assumed that at $E_m = 40$ mV: (1) $\kappa = \tau_h^{-1}$, (2) $\lambda = 0$, and (3) $(\epsilon + \pi)^{-1}$ equals the value determined by the two-pulse procedure described by Chandler and Meves, 1970 *b*, (for further details of the method see Chandler and Meves, 1970 *c*: pages 682–3). The parameters $\bar{g}_{Na}$, a and b relate to sodium channel activation and were determined to best fit the rising phase of the curve, whereas ϵ/π refers to the second open state of the channels and sets the steady-state level of the sodium conductance. In a series of measurements (not shown) the ratio $(\epsilon + \pi)^{-1}$ to τ_h was found to remain constant, independent of pH_i (Table II), and in good agreement with the value obtained by Chandler and Meves (1970 *c*).

Further support for the appropriation of the model adopted in the Appendix comes from the results of the curve fitting shown in Figs. 4 and 10. Following those arguments, we were able to fit both the pH-dependence of g^{ss}_{Na} and the time-course of g_{Na} at various pH_i. Particularly, $g_{Na}(t)$ curves were simulated by linearly combining the contributions of channels C_3 and C_2 at pH_i 9.9 and channels C_1 and C_2 at pH_i 5.4 (Appendix and Fig. 10 legend for further details). As shown in Table II, variations of κ, ϵ, and π are required to best fit the experimental points both at high and low pH_i. This does not conflict with the hypothesis of channels mixtures which at present seems to be inescapable (at least for the high pH_i), but it would rather indicate that an action of pH_i on reaction rates should also be considered. Interestingly, an attempt at curve fitting the experimental points in terms of simple changes of κ, ϵ, and π did not give reliable results.

Chemical Nature of Groups Controlling the Inactivation Gate

The existence of a titratable group with pK_a 10.4 modifying $h_\infty(E)$ is in good agreement with the suggestion of Rojas and Rudy (1976) and Eaton et al. (1978) that a basic amino acid residue, either arginine or lysine, might be involved in the inactivation gating structure. Such structure was assumed to be: (*a*) positively charged at neutral pH_i, (*b*) located nearly at the inner mouth of the Na^+ channel, and (*c*) free to move from a resting to a blocking position on depolarization. A consequence of this is that at very high pH_i a large fraction of basic residues would be in the uncharged form so that, once opened by step depolarizations most Na channels would be unable to inactivate. This seems in fairly good agreement with the results of Figs. 1–3. Sodium currents can inactivate normally at pH_i 7.2, much less at intermediate pH and not at all at pH 11.

An alternative to the "arginine-lysine hypothesis" could be that a tyrosine residue might be involved in the inactivation gating, as suggested by Oxford et el., 1978, and Brodwick and Eaton, 1978. Under these conditions, the presence on the same gating structure of the phenolic group of tyrosine (uncharged at neutral pH) and the guanidino group of arginine (positively charged at pH 11) would give origin to a short peptide chain positively charged at neutral pH and uncharged at pH 11 where the phenolic group of tyrosine is in the anionic form. Of course, other aminoacid combinations and/or totally different mechanisms could account reasonably well for the above data. Further experiments are required to clarify this point.

TABLE II

PARAMETERS OF THE THEORETICAL CURVES IN FIG. 10

pH	*a*	*b*	*k*	λ	ϵ	π	g_{Na}	C_1	C_2	C_3
				ms^{-1}			$mS \cdot cm^{-2}$		%	
7.2	6.5	0.05	0.54	0	0.16	1.09	47	0	100	0
9.9	5.5	0.1	0.32	0	0.164	746	33	0	42	0
	5.5	0.1	0	0	0	0	33	0	0	58
5.4	3.5	0.2	0.48	0	0.26	1.2	31	0	32	0
	3.5	0.2	0.48	0	0	0	31	68	0	0

Very little is known about the nature of the side-group titrating at low pH_i ($pK_a = 5.6$). From the pK_a of the titration curve it is difficult to argue which type of amino acid residue is implicated in the potentiation of sodium inactivation. Carboxyl groups of aspartic and glutamic acid as well as the imidazole group of hystidine might titrate in that pH range. In addition, the lack of other papers reporting implications of protein side-groups in the control of ϵ and π suggests some caution in drawing general conclusions from the present data.

An important aspect of the H^+ inactivation interaction is the decrease above -20 mV of the rate of inactivation with increasing pH_i. An explanation for this could be that, because protonation-deprotonation reactions are very fast, the groups responsible for the Na inactivation would acquire a positive charge which on average decreases with increasing the pH_i ($+e$ at pH_i 7.2 and 0 at pH_i 12). Thus, if one assumes that the rate κ is somehow related to the average charge of those groups, it would follow that the time required by channel to go from the open (x_1) to the closed state ($x_1 z$) would increase at high pH_i. The contrary would be true for lowering the pH_i. Of course, the hypothesis deserves further investigation; especially on the view that other chemical agents and toxins can easily affect the time-course of fast inactivation (Meves, 1978; Catterall, 1979; Oxford and Swenson, 1979).

Actions on Membrane Surface Charges

An interesting finding of this paper is that, besides horizontal shifts, the kinetic parameters of both Na^+ and K^+ channels apparently show also vertical shifts upon altering the intracellular pH. In terms of the Eyring rate theory (Glasstone et al., 1941) this would suggest that H^+ ions affect both the electrostatic and the nonelectrostatic free-energy terms associated with the activation rate constants. A tentative separation of the two phenomena based on an empirical procedure has been shown in Figs. 8 and 9. Obviously, the method suffers serious limitations and thus, for the vertical shifts, we thought it more realistic to discuss the qualitative aspects of some plausible mechanism accounting for the observed shifts rather then furnishing a quantitative interpretation of the phenomenon. For the horizontal shifts the matter is simplified by the observation that other parameters show also voltage shifts in the same direction (h_∞, g^p_{Na} and g_K). As described below, they can be satisfactorily explained in terms of the Gouy-Chapman-Stern equation applied to the diffuse double layer generated by the fixed membrane surface charges (Gilbert and Ehrenstein, 1969; Hille et al., 1975).

HORIZONTAL SHIFTS Three main pieces of experimental evidence suggested to us a model (Fig. 5, legend) with a minimum of three different surface charges: (*a*) the shift toward depolarizing voltages of g_K, g^p_{Na}, α_n and a at high pH_i, (*b*) the shift toward hyperpolarizing voltages of $h_\infty(E)$ at low pH_i and (*c*) the existence at the internal side of the membrane of a net negative charge at pH_i 7.2 (Chandler et al., 1965). Points *a* and *b* are fairly well satisfied by assuming the existence of a basic group with pK_a 9–10 (pK_3) and an acid group with pK_a 4.5 (pK_1) while the need for a second type of negative charge with pK_a 2.8 (pK_2) is merely imposed by the third constraint for which the total surface charge ($\sigma_1 + \sigma_2 + \sigma_3$) has to be negative at pH_i 7.2.

The fitting of the ΔV shifts shown in Figs. 5, 7, and 9 was carried out by simple trial and error assuming for the variable B a value of 20 mV, in agreement with Chandler et al., 1965, that estimated a value of 17 mV for axons perfused with 300 mM KCl. Under these conditions, the results from both Na^+ and K^+ channels would suggest that on the internal

surface of the squid axon membrane there would exist possibly three types of surface charges. They would be tentatively associated with carboxyl (pK_1 4.5), phosphate (pK_2 2.8), and amino (pK_3 9–10) groups, furnishing a total negative surface charge of 1.5×10^{-3} electronic charges $Å^{-2}$, corresponding to a linear separation of 26 Å (in good agreement with the value of 27 Å obtained by Chandler et al., 1965). However, some ambiguity remains as to the reason why we failed to detect clear shifts of g_K and α_n(or g^p_{Na} and a) toward hyperpolarizing voltages at low pH_i. For this reason and because of the lack of systematic studies changing the ionic strength and the divalent ion concentration, the present results should be considered as mainly indicative.

VERTICAL SHIFTS The simplest way in which vertical shifts of the kinetic parameters can be produced is by changing the temperature of the solution bathing the axon (Frankenhaeuser and Moore, 1963; Schauf, 1973). For the case of pH_i, there are at least two possibilities (not necessarily mutually exclusive) in which this might occur: either the pH alters considerably the fluidity of the lipid bilayer or it affects the activation gating mechanism by modifying the average charge of some titratable group associated with the gate. In favor of the first possibility, evidence has been accumulated (Traüble and Eibl, 1974; Verkleij et al., 1974; Watts et al., 1978; Eibl and Blume, 1979) on the effects that H^+ ions produce on the ordered fluid-phase transition temperature of lipid bilayers, suggesting that when the phospholipid head groups are mostly uncharged (protonated), the fluidity of the membrane is lower because of the decreased intermolecular separation caused by the lower electrostatic repulsion. On a macroscopic scale, this would produce effects similar to lowering the temperature (slowing down of rate constants) with an action that would be symmetric with respect to the plane of the membrane and common to both types of channels. Interestingly, this would account also for the effects of low pH_o on α_n and α_m (Carbone et al., 1978) which have been found to produce not simple horizontal shifts of the two quantities.

The alternative possibility that pH_i could affect the rate of opening and closing of channels by acting directly on the gating mechanism should also be considered (Shrager, 1974). If, for instance, the rate of opening and closing of the activation gate is assumed to be controlled by the degree of protonation of some acid group, one would predict that at low pH when the group is uncharged for a greater fraction of time, the time required by the gate to move from the closed to the open position would increase. Obviously, to account for the similar effects that pH_i and pH_o have on Na^+ and K^+ channels, analogous residues should be postulated to exist at the two sides of both types of channels.

CONCLUSIONS

For the sake of clarity, we thought useful to list in Table III the pK_a values of the most probable groups associated with the various voltage-clamp variables of the squid axon membrane. From the table it appears that at the extracellular side of the membrane there are no basic residues affecting either one of the listed parameters. This would suggest two orders of considerations. First, amino, imidazole, and sulfhydryl groups are not very likely accessible at the outer side of the axolemma. Second, the squid axon membrane seems to be characterized by a high degree of asymmetry on its membrane constituents (Zambrano et al., 1971). Significantly, the steady-state sodium inactivation is the only parameter affected by residues having the same pK_a on both sides of the membrane.

TABLE III

TITRATABLE GROUPS ASSOCIATED WITH VOLTAGE-CLAMP PARAMETERS

	Internal		External	
	pK_a	Reference	pK_a	Reference
Na				
Maximum conductance $\bar{g}_{Na}$ (block)	5.8	Wanke et al., 1980	4.6	Wanke et al., 1980
Peak conductance $g_{Na}(E)$ (shift)	9.9	Fig. 5	4.5*	Carbone et al., 1978
Steady-state conductance, g^{ss}_{Na}(ampl)	5.6 and 10.4	Fig. 4 and Brodwick and Eaton, 1978	—	—
Activation rates, $a(E)$, $\alpha_m(E)$ (shift)	9.5–10‡	Fig. 8	4.5	Carbone et al., 1978
Inactivation, $h_\infty(E)$ (shift)	4.5	Fig. 6	4–5‡	Carbone et al., 1978 (Fig. 5)
K				
Maximum conductance $\bar{g}_K$ (block)	6.4	Wanke et al., 1979	3.4§	This paper
Steady-state conductance, $g_K(E)$ (shift)	9	Fig. 9	4.7*	Carbone et al., 1978
Activation rate, $\alpha_n(E)$ (shift)	9–9.5‡	Fig. 9	4.7	Carbone et al., 1978

*The group is reported to be similar to the group associated with the corresponding activation rate.
‡The pK_a of this group is determined qualitatively from the figure indicated.
§The group is only stated to exist in this paper (Results).

In our opinion it is extremely difficult, at present, to furnish a correct topology of the discovered titratable groups. Perhaps, with reasonable caution, one might conclude that the amino acid residues controlling $\bar{g}_{Na}$ (Wanke et al., 1980), $\bar{g}_K$ (Wanke et al., 1979) and g^{ss}_{Na} (Fig. 4) are possibly located nearly the channel mouth. On the contrary, very little can be inferred about those groups controlling the voltage shifts of the remaining variables. For this, more information concerning both the lipid-proteins interactions (Warren et al., 1974) and the nature of the voltage-sensitive channel gating would be required. Along this line, experiments designed to measure gating signals as a function of pH are in progress.

APPENDIX

We will give here a brief description of the theoretical model adopted to fit the experimental data of Figs. 4 and 10. The model is based on the assumption that:

(*a*) There are three types of channels C_1, C_2, C_3 at various pH_i in rapid equilibrium with each others, having respectively the following reaction scheme:

$$(C_1) \qquad x_3 \underset{b}{\overset{a}{\rightleftharpoons}} x_2 \underset{b}{\overset{a}{\rightleftharpoons}} x_1 \xrightarrow{\kappa} x_1 z$$

$$(C_2) \qquad x_3 \underset{b}{\overset{a}{\rightleftharpoons}} x_2 \underset{b}{\overset{a}{\rightleftharpoons}} x_1 \xrightarrow{\kappa} x_1 z \underset{\pi}{\overset{\epsilon}{\rightleftharpoons}} h_2$$

$$(C_3) \qquad x_3 \underset{b}{\overset{a}{\rightleftharpoons}} x_2 \underset{b}{\overset{a}{\rightleftharpoons}} x_1,$$

where x_3 and x_2 represent the resting closed state of the channel and a,b are rate constants. For computational reasons, only two rather than three closed states are considered. The other quantities are defined in the text.

(*b*) The populations of C_1, C_2, C_3, are governed by two independent first-order chemical reactions, with dissociation constants K_a and K_b:

$$C_2 + H^+ \overset{K_a}{\rightleftharpoons} C_1$$

$$C_3 + H^+ \overset{K_b}{\rightleftharpoons} C_2$$

furnishing the following relations:

$$[C_1] = [C_2] \cdot 10^{pK_a - pH} \tag{1}$$

$$[C_2] = [C_3] \cdot 10^{pK_b - pH} \tag{2}$$

(*c*) The two open states x_1 and h_2 have the same single-channel conductance (Chandler and Meves, 1970 *b*; Bezanilla and Armstrong, 1977) whereas state $x_1 z$ is nonconducting.

(*d*) The total number of channels $[C_1] + [C_2] + [C_3]$ is constant at any pH.

Under these hypotheses the steady-state sodium conductance at a given pH will be the sum of the contributions of the channels C_2 and C_3. For large values of t all C_1 are inactivated and therefore do not contribute to g^{ss}_{Na}. Hence:

$$g^{ss}_{Na}(pH) = (g^{n}_{Na}[C_2] + g^{m}_{Na}[C_3])/([C_1] + [C_2] + [C_3]), \tag{3}$$

where g^{n}_{Na} and g^{m}_{Na} indicate the conductance that would have been obtained if all channels were either of the C_2 or C_3 type.

Substituting Eqs. 1 and 2 into 3 we obtain:

$$g^{ss}_{Na}/g^{m}_{Na} = (1 + 10^{pK_a - pH} + 10^{pH - pK_b})^{-1} \cdot [10^{pH - pK_b} + (g^{n}_{Na}/g^{m}_{Na})]. \tag{4}$$

Assuming $g^{m}_{Na} = g^{\ell}_{Na}$ at pH_i 7.2, the ratio g^{ss}_{Na}/g^{m}_{Na} becomes $g^{ss}_{Na}/g^{\ell}_{Na} = I^{ss}_{Na}/I^{\ell}_{Na}$; the latter being the quantity plotted on the ordinate of Fig. 4. Indeed, the theoretical value of g^{m}_{Na} is nearly 20% higher than the experimental g^{ℓ}_{Na} (Bezanilla and Armstrong, 1977). Thus the above assumption would introduce a comparable distortion in the pH dependence of Eq. 4. Such an error, however, is of the same order of magnitude of the scattering of our data and it would introduce only negligible deviations in the actual values of pK_b and pK_a.

The solid line in Fig. 4 is the results of a best-fitting analysis of the experimental data with Eq. 4 for $g^{n}_{Na}/g^{m}_{Na} = g^{n}_{Na}/g^{\ell}_{Na} = I^{n}_{Na}/I^{\ell}_{Na} = 0.27$, $pK_a = 5.4$ and $pK_b = 10.4$. From these values it derives that $I^{ss}_{Na}(pH)$ equals I^{n}_{Na} at pH_i 7.7.

A preliminary report of some of these experiments was presented at the EMBO (European Molecular Biology Organization) Workshop on Polypeptide Neurotoxins, Nice (France), 1979.

We would like to thank Dr. Hans Meves, Dr. Bertil Hille, and Dr. Franco Conti for reading the manuscript and offering valuable suggestions, Dr. Paolo Gazzotti for suggesting us the possibility of the pH-dependent bilayer fluidity. The technical assistance of Mr. F. Pittaluga and secretarial help of Miss O. Graffigna are gratefully acknowledged.

Received for publication 29 July 1980 and in revised form 10 March 1981.

REFERENCES

Armstrong, C. M., and F. Bezanilla. 1977. Inactivation of the sodium channel. II. Gating current experiments. *J. Gen. Physiol.* 70:567–590.

Armstrong, C. M., F. Bezanilla, and E. Rojas. 1973. Destruction of sodium conductance inactivation in squid axons perfused with Pronase. *J. Gen. Physiol.* 62:375–391.

Atwell, D., and D. Eisner. 1978. Discrete membrane surface charge distributions. Effects of fluctuations near individual channels. *Biophys. J.* 24:869–875.

Bezanilla, F., and C. M. Armstrong. 1972. Negative conductance caused by entry of sodium and cesium ions into potassium channels of squid axons. *J. Gen. Physiol.* 60:588–608.

Bezanilla, F., and C. M. Armstrong. 1977. Inactivation of the sodium channel. I. Sodium current experiments. *J. Gen. Physiol.* 70:549–566.

Binstock, L., W. J. Adelman, Jr., J. P. Senft, and H. Lecar. 1975. Determination of the resistance in series with the membranes of giant axons. *J. Membr. Biol.* 21:25–47.

Brodwick, M. S., and D. C. Eaton. 1978. Sodium channel inactivation in squid axon is removed by high internal pH or tyrosine-specific reagents. *Science (Wash. D.C.).* 200:1494–1496.

Campbell, D. T., and B. Hille. 1976. Kinetic and pharmacological properties of the sodium channel of frog skeletal muscle. *J. Gen. Physiol.* 67:309–323.

Carbone, E., R. Fioravanti, G. Prestipino, and E. Wanke. 1978. Action of extracellular pH on Na^+ and K^+ membrane currents in the giant axon of *Loligo vulgaris*. *J. Membr. Biol.* 43:295–315.

Catterall, W. A. 1979. Binding of scorpion toxin to receptor sites associated with sodium channels in frog muscle. Correlation of voltage-dependent binding with activation. *J. Gen. Physiol.* 74:375–391.

Chandler, W. K., A. L. Hodgkin, and H. Meves. 1965. The effect of changing the internal solution on sodium inactivation and related phenomena in giant axons. *J. Physiol. (Lond.).* 180:821–836.

Chandler, W. K., and H. Meves. 1965. Voltage clamp experiments on internally perfused giant axons. *J. Physiol. (Lond.).* 180:788–820.

Chandler, W. K., and H. Meves. 1970 *a*. Sodium and potassium currents in squid axons perfused with fluoride solutions. *J. Physiol. (Lond.).* 211:623–652.

Chandler, W. K., and H. Meves. 1970 *b*. Evidence for two types of sodium conductance in axons perfused with sodium fluoride solutions. *J. Physiol. (Lond.).* 211:653–678.

Chandler, W. K., and H. Meves. 1970 *c*. Rate constants associated with changes in sodium conductance in axons perfused with sodium fluoride. *J. Physiol. (Lond.).* 211:679–705.

Chandler, W. K. and H. Meves. 1970 *d*. Slow changes in membrane permeability and long-lasting action potentials in axons perfused with fluoride solutions. *J. Physiol. (Lond.).* 211:707–728.

Courtney, K. R. 1979. Extracellular pH selectively modulates recovery from sodium inactivation in frog myelinated nerve. *Biophys. J.* 28:363–368.

Drouin, H., and B. Neumcke. 1974. Specific and unspecific charges at the sodium channels of the nerve membrane. *Pfluegers Arch. Eur. S. Physiol.* 351:207–229.

Eaton, D. C., G. S. Oxford, M. S. Brodwick, and B. Rudy. 1978. Arginine-specific reagents remove sodium channel inactivation. *Nature (Lond.).* 271:473–475.

Ehrenstein, G., and H. M. Fishman. 1971. Evidence against hydrogen-calcium competition model for activation of electrically excitable membranes. *Nature (Lond.).* 233:16–17.

Eibl, H., and A. Blume. 1979. The influence of charge on phosphatidic acid bilayer membranes. *Biochim. Biophys. Acta.* 553:476–488.

Frankenhaeuser, B., and A. L. Hodgkin. 1956. The after-effect of impulses in the giant nerve fibers of Loligo. *J. Physiol. (Lond.).* 131:341–359.

Frankenhaeuser, B., and L. E. Moore. 1963. The effect of temperature of the sodium and potassium permeability changes in myelinated nerve fibres of *Xenopus laevis*. *J. Physiol. (Lond.).* 169:431–437.

French, R. J., and J. B. Wells. 1977. Sodium ions as blocking agents and charge carriers in the potassium channel of the squid giant axon. *J. Gen. Physiol.* 70:707–724.

Gilbert, D. L., and G. Ehrenstein. 1969. Effect of divalent cations on potassium conductance of squid axons. Determination of surface charge. *Biophys. J.* 9:447–463.

Glasstone, S., K. J. Laidler, and H. Eyring. 1941. The theory of rate processes. McGraw-Hill Book Company, New York.

Hille, B. 1968. Charges and potentials at the nerve surface. Divalent ions and pH. *J. Gen. Physiol.* 51:221–236.

Hille, B., A. M. Woodhull, and B. I. Shapiro. 1975. Negative surface charge near sodium channels of nerve: divalent ions, monovalent ions, and pH. *Philos. Trans. R. Soc. Lond. B Biol. Sci.* 207:301–318.

Hodgkin, A. L., and A. F. Huxley. 1952 *a*. The dual effect of membrane potential on sodium conductance in the giant axon of Loligo. *J. Physiol. (Lond.)*. 116:497–506.

Hodgkin, A. L., and A. F. Huxley. 1952 *b*. A quantitative description of membrane current and its application to conduction and excitation in nerve. *J. Physiol. (Lond.)*. 117:500–544.

Meves, H. 1978. Inactivation of the sodium permeability in squid giant fibres. *Prog. Biophys. Mol. Biol.* 33:207–230.

Mozhayeva, G. N., and A. P. Naumov. 1970. Effect of surface charge on the steady-state potassium conductance of nodal membrane. *Nature (Lond.)*. 228:164–165.

Nonner, W., B. C. Spalding, and B. Hille. 1980. Low intracellular pH and chemical agents slow inactivation gating in sodium channels of muscle. *Nature (Lond.)*. 284:360–363.

Ohmori, H., and M. Yoshii. 1977. Surface potential reflected in both gating and permeation mechanisms of sodium and calcium channels of the tunicate egg cell membrane. *J. Physiol. (Lond.)*. 267:429–463.

Oxford, G. S., C. H. Wu, and T. Narahashi. 1978. Removal of sodium channel inactivation in squid giant axons by *N*-bromoacetamide. *J. Gen. Physiol.* 71:227–247.

Oxford, G. S., and R. P. Swenson. 1979. *n*-Alkanols potentiate sodium channel inactivation in squid giant axons. *Biophys. J.* 26:585–590.

Rojas, E., and B. Rudy. 1976. Destruction of the sodium conductance inactivation by a specific protease in perfused nerve fibres from *Loligo*. *J. Physiol. (Lond.)*. 262:501–531.

Schauf, C. L. 1973. Temperature dependence of the ionic current kinetics of *Myxicola* giant axons. *J. Physiol. (Lond.)*. 235:197–205.

Schauf, C. L., and J. O. Bullock. 1978. Internal cesium alters sodium inactivation in *Myxicola*. 23:473–477.

Schauf, C. L., and F. A. Davis. 1976. Sensitivity of the sodium and potassium channels of Myxicola giant axons to changes in external pH. *J. Gen. Physiol.* 67:185–195.

Shrager, P. 1974. Ionic conductance changes in voltage-clamped crayfish axons at low pH. *J. Gen. Physiol.* 64:666–690.

Tasaki, I., I. Singer, and T. Takenaka. 1965. Effects of internal and external environment on excitability of squid giant axon. A macromolecular approach. *J. Gen. Physiol.* 48:1095–1103.

Träuble, H., and H. Eibl. 1974. Electrostatic effects on lipid phase transitions: membrane structure and ionic environment. *Proc. Natl. Acad. Sci. U.S.A.* 71:214–219.

Verkleij, A. J., B. De Kruyff, P. H. J. T. Ververgaert, J. F. Tocanne, and L. L. M. Van Deenen. 1974. The influence of pH, Ca^{2+} and protein on the thermotropic behaviour of the negatively charged phospholipid, phosphotidylglycerol. *Biochim. Biophys. Acta*. 339:432–437.

Wanke, E., E. Carbone, and P. L. Testa. 1978. Internal pH effects on the membrane of the squid giant axon. *Int. Congr. Biophys. Abstr. (Kyoto)*. 1:152. (Abstr.)

Wanke, E., E. Carbone, and P. L. Testa. 1979. K^+-conductance modified by a titratable group accessible to protons from the intracellular side of the squid axon membrane. *Biophys. J.* 26:319–324.

Wanke, E., E. Carbone, and P. L. Testa. 1980. The sodium channel and intracellular H^+ blockage in squid axons. *Nature (Lond.)*. 287:62–63.

Warren, G. B., P. A. Toon, N. J. M. Birdsall, A. G. Lee, and J. C. Metcalfe. 1974. Reversible lipid transitions of the activity of pure adenosine triphosphatase-lipid complexes. *Biochemistry*. 13:5501–5507.

Watts, A., K. Harlos, W. Maschke, and D. Marsh. 1978. Control of the structure and fluidity of phosphotidylglycerol bilayers by pH titration. *Biochim. Biophys. Acta*. 510:63–74.

Woodhull, A. M. 1973. Ionic blockage of sodium channels in nerve. *J. Gen. Physiol.* 61:687–708.

Yeh, J. Z., and T. Narahashi. 1977. Kinetics analysis of pancuronium interaction with sodium channels in squid axon membranes. *J. Gen. Physiol.* 69:293–323.

Zambrano, F., M. Cellino, and M. Canessa-Fischer. 1971. The molecular organization of nerve membranes. IV. The lipid composition of plasma membranes from squid retinal axons. *J. Membr. Biol.* 6:289–303.